

Angle-resolved photoemission study of Nb-doped SrTiO₃

M. Takizawa, K. Maekawa, H. Wadati, T. Yoshida, and A. Fujimori
Department of Physics, University of Tokyo, Bunkyo-ku, Tokyo 113-0033, Japan

H. Kumigashira and M. Oshima
Department of Applied Chemistry, University of Tokyo, Bunkyo-ku, Tokyo 113-8656, Japan
 (Received 15 December 2008; published 18 March 2009)

We have performed an angle-resolved photoemission spectroscopy (ARPES) study of the O $2p$ valence-band structure of Nb-doped SrTiO₃, in which a dilute concentration of electrons are doped into the d^0 band insulator. We have found that ARPES spectra at the valence-band maxima at the M [$\mathbf{k}=(\frac{\pi}{a}, \frac{\pi}{a}, 0)$] and R [$\mathbf{k}=(\frac{\pi}{a}, \frac{\pi}{a}, \frac{\pi}{a})$] points start from ~ 3.3 eV below the Fermi level (E_F), consistent with the indirect band gap of 3.3 eV and the E_F position at the bottom of the conduction band. The peak position of the ARPES spectra were, however, shifted toward higher binding energies by ~ 500 meV from the 3.3 eV threshold. Because the bands at the M and R points have pure O $2p$ character, we attribute this ~ 500 meV shift to strong coupling of the oxygen p hole with optical phonons, in analogy with the peak shifts observed for d -electron photoemission spectra in various transition-metal oxides.

DOI: [10.1103/PhysRevB.79.113103](https://doi.org/10.1103/PhysRevB.79.113103)

PACS number(s): 71.38.-k, 71.20.-b, 71.28.+d, 79.60.-i

Transition-metal oxides are known to exhibit a variety of attractive phenomena such as high-temperature superconductivity, giant magnetoresistance, and metal-insulator transition¹ resulting from interaction among the transition-metal $3d$ electrons. Among transition-metal oxides, perovskite-type Ti and V oxides are ideal systems to study the fundamental physics of electron correlation because they are prototypical Mott-Hubbard-type systems. So far, their electronic structures have been modeled by the Hubbard model without an explicit consideration of oxygen p orbitals. Recently, extended cluster-model analysis of $\text{Ca}_{1-x}\text{Sr}_x\text{VO}_3$ has suggested that contributions from the O $2p$ states are significant in the correlated V $3d$ bands.² Also resonant photoemission spectroscopy (PES) study of Nb-doped SrTiO₃ (STO) has revealed that the electron-doping induced states are not simple Ti $3d$ states but are strong hybridized states of Ti $3d$ and O $2p$.³ STO is a perovskite-type $3d^0$ band insulator with the filled O $2p$ band and the empty Ti $3d$ band. The band gap (E_g) of STO determined by optical measurements is ~ 3.3 eV for the indirect gap and ~ 3.8 eV for the direct gap.^{4,5} Substituting La for Sr, Nb for Ti, or introducing oxygen vacancies leads to electron doping and makes the system metallic and even superconducting already from very low carrier concentrations of $8.5 \times 10^{18} \text{ cm}^{-3}$.^{6,7} The band structure has been studied theoretically by many groups.^{5,8-10} Angle-resolved photoemission spectroscopy (ARPES) measurements have also been performed^{11,12} to study the band structure of STO, however, these measurements were made for several k points in the Brillouin zone, mainly using the so-called normal-emission method.

In the present work, we have made detailed ARPES measurements on Nb-doped, i.e., lightly electron-doped, STO and have examined the dispersions of the O $2p$ band and the bottom of the Ti $3d$ band. The dispersions of the O $2p$ band has been well explained by tight-binding (TB) band-structure calculation if the band gaps are adjusted to the optical gaps of 3.3 and 3.8 eV. Photoemission starts from ~ 3.3 eV below the Fermi level (E_F), consistent with the indirect optical gap of 3.3 eV. However, the ARPES peak positions of the O $2p$

bands are located ~ 500 meV below the valence-band maximum (VBM). We attribute the 500 meV shift to the coupling of the O $2p$ hole to optical phonons.

ARPES measurements were performed at BL-1C of Photon Factory, High Energy Accelerators Research Organization (KEK). A Nb-doped STO single crystal with an atomically flat (001) surface of TiO₂ termination was measured.¹³ To introduce carriers (electrons) into the sample, it was annealed under an ultrahigh vacuum ($\sim 1 \times 10^{-9}$ Torr) at 1273 K for 2 h, and then transferred to the photoemission chamber without exposing it to air.¹⁴ The amount of the doped carriers was so small that changes in the band structure are considered to be negligible from those of the pure STO. Measurements were performed in an ultrahigh vacuum of $\sim 1 \times 10^{-10}$ Torr at 20 K using a Scienta SES-100 electron-energy analyzer. The total-energy resolution including the monochromator was set to ~ 60 and ~ 150 meV near E_F and in the valence-band region, respectively. The E_F position was determined by measuring gold spectra. Traces in momentum space for changing emission angle are shown in the right panels of Fig. 1, when the widths represent the k_z broadening due to the finite escape depth of photoelectrons.¹⁵ In order to calculate the momentum perpendicular to the sample surface, we have assumed the free-electron-like final states, and used the work function of the sample $\phi=4.1$ eV, the inner potential $V_0=17$ eV, and the lattice constant $a=3.905$ Å.

Figures 1(a)–1(c) show energy distribution curves (EDCs) taken with photon energies of 86 and 58 eV, showing clear band dispersions. In order to see the band dispersions more clearly, we have taken the second derivatives of the EDCs and plotted them on a gray scale in Figs. 1(d)–1(f). Here, bright part indicates peaks or shoulders in the EDCs. In Fig. 2(a), the E - k intensity plot near E_F around the Γ point is shown. The intensity in the vicinity of E_F arises from the bottom of the Ti $3d$ band, which is occupied by a small amount of electrons doped into the sample. From the size of the occupied part in momentum space ($|k_F| \sim 0.15 \frac{\pi}{a}$), the carrier density is estimated to be $\sim 1 \times 10^{-2}$ per Ti atoms by

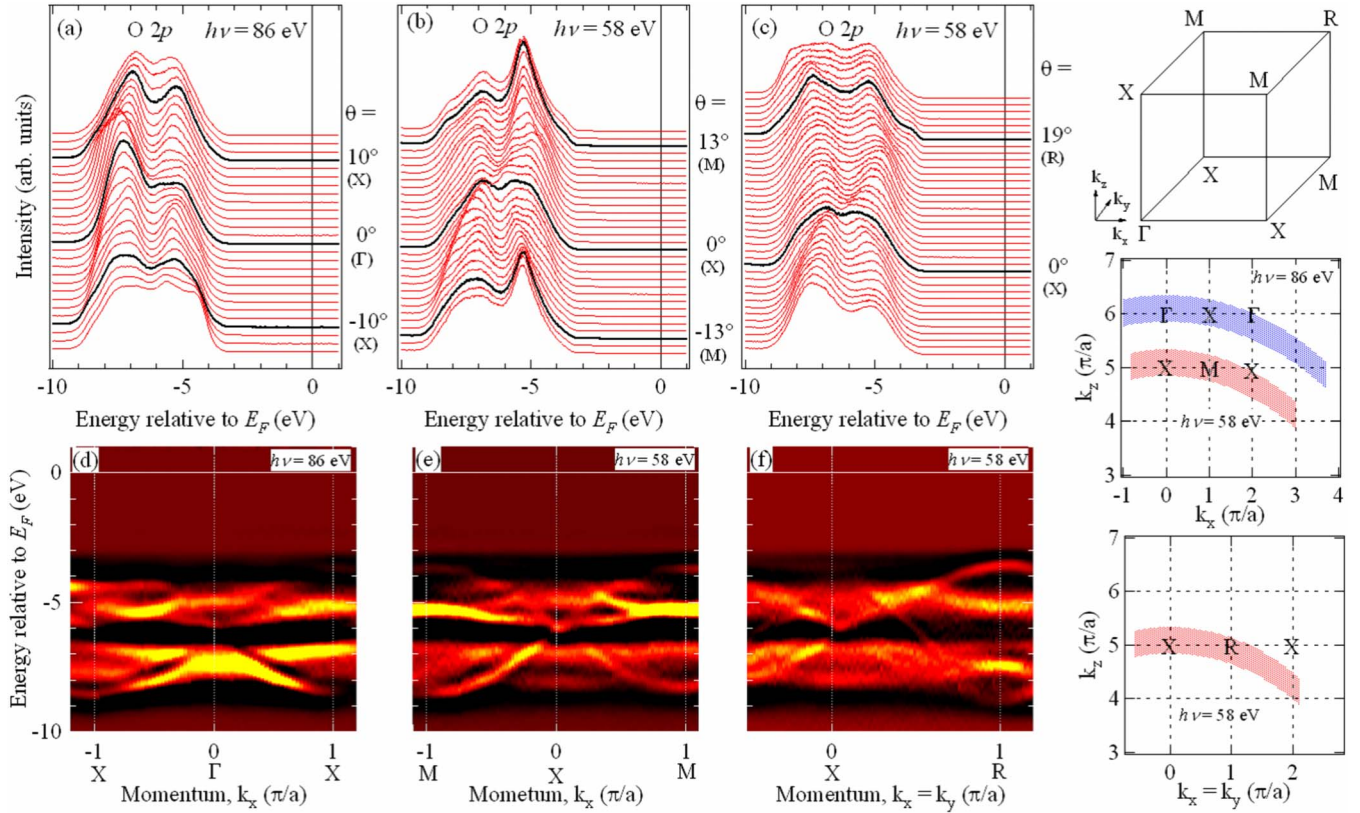


FIG. 1. (Color online) ARPES spectra of SrTiO₃. [(a)–(c)] EDCs taken with photon energies $h\nu=86$ eV and $h\nu=58$ eV. [(d)–(f)] Grayscale plots of the second derivatives of the EDCs for the Γ -X direction, the X-M direction, and the X-R direction. Here, bright parts correspond to energy bands. Right top: Brillouin zone of the simple cubic lattice. Right middle and bottom: traces in momentum space for $h\nu=86$ eV and 58 eV and emission angle from $\theta=-10^\circ$ to 40° .

assuming the Fermi surface to be threefold degenerate spheres of the t_{2g} bands. Then, the Fermi energy is estimated to be as small as ~ 40 meV from the above $|k_F|$ value and the effective mass $m^*=1.5m_0$,¹¹ where m_0 is the free-electron mass. Therefore, the Fermi level is located only ~ 40 meV above the bottom of the Ti 3d-derived conduction band. The EDCs at the M point [$\mathbf{k}=(\frac{\pi}{a}, \frac{\pi}{a}, 0)$] and the R point [$\mathbf{k}=(\frac{\pi}{a}, \frac{\pi}{a}, \frac{\pi}{a})$], both corresponding to the top of the O 2p band of pure O 2p character, are shown in Figs. 2(b) and 2(c). The emission starts at the threshold of ~ 3.3 eV below E_F , that is, 3.3 eV below the bottom of Ti 3d band. The value of 3.3 eV is equal to the magnitude of the indirect band gap of STO between the valence-band maximum at the M or R point and the conduction-band minimum at the Γ point. Both spectra have been decomposed into several Gaussians, out of which the lowest-binding-energy ones are shown in Figs. 2(b) and 2(c). Thus, the peak position of the lowest-binding-energy Gaussian is observed 3.8 eV below E_F , i.e., by ~ 500 meV deeper than the threshold.

In order to interpret the experimental band dispersions quantitatively, the ARPES spectra have been fitted to TB band-structure calculation. We have performed the TB calculation including the Ti 3d and O 2p orbitals (totally, 14 atomic orbitals) as the basis set.^{8–10} Parameters to be adjusted are the energy difference between the Ti 3d and O 2p levels, $\epsilon_p - \epsilon_d$, the crystal-field splitting of the O 2p orbitals, $\epsilon_{p\sigma} - \epsilon_{p\pi}$, and Slater-Koster parameters ($pd\sigma$), ($pd\pi$), ($pp\sigma$),

and ($pp\pi$).¹⁶ We chose the TB parameters to reproduce the observed band dispersions as well as the indirect and direct optical band gaps of 3.3 and 3.8 eV, respectively,⁵ as shown in Fig. 3(a). Best-fit parameters are $\epsilon_p - \epsilon_d = -5.7$ eV, $\epsilon_{d\sigma} - \epsilon_{d\pi} = 2.2$ eV, $\epsilon_{p\sigma} - \epsilon_{p\pi} = 1.5$ eV, ($pd\sigma$) = -2.3 eV, ($pp\sigma$) = 0.40 eV. Also, we assumed ($pd\pi$) = $-0.46(pd\sigma)$, ($pp\pi$) = $-0.25(pp\sigma)$.¹⁷ Here, the same shift of ~ 500 meV between the ARPES peaks and the TB band dispersions are assumed not only at the VBM at the M and R points but also over the entire O 2p bands, although the shifts may differ between the bands and k points. As shown in Figs. 3(b)–3(d), the calculated band dispersions could successfully reproduce the experimental dispersions of peak positions in the EDCs, except for the overall shift of ~ 500 meV between the ARPES data and the TB calculation. Some of the bands which cannot be reproduced in the calculation may come from the surface reconstructed layer, which was observed by low-energy electron-diffraction pattern. Here, it should be noted again that the shift of E_F due to electron doping is as small as ~ 40 meV as mentioned above. Furthermore, according to the previous PES measurement of La_{1-x}Sr_xTiO₃,¹⁸ electron doping into STO induces chemical-potential shifts as small as ~ 200 meV from STO to LaTiO₃ (100% electron doping). Therefore, electron doping caused by the oxygen vacancies and/or Nb substitution cannot explain the energy shift as large as ~ 500 meV.

In order to explain the discrepancies between the ARPES peak dispersion and the TB band structure fitted to the opti-

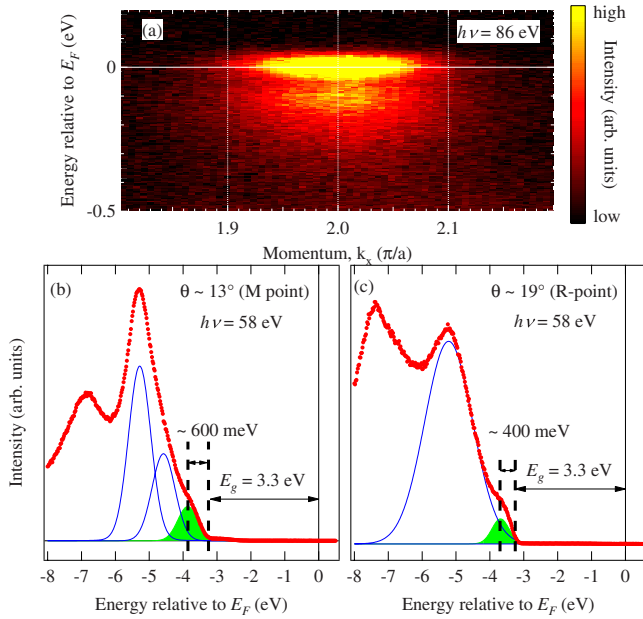


FIG. 2. (Color online) ARPES spectra of SrTiO₃. (a) Intensity plot in E - k space around the Γ point. The bottom of the Ti 3d band was observed at the Γ point in the vicinity of E_F . [(b), and (c)] EDCs at the M point and the R point. They have been decomposed into several Gaussians, out of which only a few lowest-binding-energy ones are shown.

cal band gaps, we suggest that the effect of strong electron-phonon coupling on the spectral line shape is important for the O 2p band, too. We note that the VBM at the M and R points have pure O 2p character without admixture of Ti 3d. In the scenario of strong electron-phonon coupling effect on photoemission spectra, strong multiple phonon peaks appear on the higher-binding-energy side of the weak (almost invisible) zero-phonon line, making the spectral line shape broad and apparently shifted toward higher binding energies by the multiple phonon energy compared with the zero-phonon peak (threshold).¹⁹ Therefore, ARPES peaks will be observed at higher binding energies than the optical band gap suggests. In the photoemission spectra of several transition-metal oxide (TMOs), such effects of electron-phonon coupling have been

reported in 3d-electron photoemission spectra. For example, in the case of Ca₂CuO₂Cl₂, the energy shift between the photoemission threshold and the photoemission peak is found to be ~ 450 meV,²⁰ and in the case of La_{1-x}Sr_xFeO₃ ~ 1 eV.²¹ When an electron is strongly coupled with optical phonon modes of energy ω ,²² the energy shift is given by $\Delta = g\omega$, where g is the electron-phonon coupling constant. g can be much larger than one judged from the large energy shift compared to the maximum phonon energy = 70 meV. In order to evaluate the electron-phonon coupling constant, temperature-dependent ARPES measurements would be desired in future. It is interesting to note that we have observed effects of similar magnitude for the emission of an O 2p electron, which are generally thought to be itinerant weakly correlated. The electron-phonon coupling effects of similar magnitudes between the transition-metal 3d and O 2p electrons mean that holes in the O 2p band have tendency to be localized like a hole in the TM 3d bands.²¹ In fact, it has been known for transparent oxide semiconductors that n -type samples are much more conductive and p -type conductors had not been realized until CuAlO₂ was discovered.²³

In summary, we have performed detailed ARPES measurements of Nb-doped (lightly electron-doped) STO and have observed the ARPES peak dispersions of the O 2p band and the bottom of the Ti 3d band. The photoemission threshold at the valence-band maxima (the R and M points in the Brillouin zone) were observed at 3.3 eV below E_F , in agreement with the optical band gap. The corresponding photoemission peak, however, was found ~ 500 meV below the threshold. We interpret the shift of the ARPES peak of ~ 500 meV as an effect of strong electron-phonon coupling in analogy with the similar behaviors of d -derived photoemission peak in insulating 3d TMOs.

This work was supported by a Grant-in-Aid for Scientific Research (Grant No. 19204037) from JSPS and that for Priority Area “Invention of Anomalous Quantum Materials” (Grant No. 16076208) from MEXT, Japan. The work at KEK-PF was done under the approval of Photon Factory Program Advisory Committee (Proposal No. 2005S2-002).

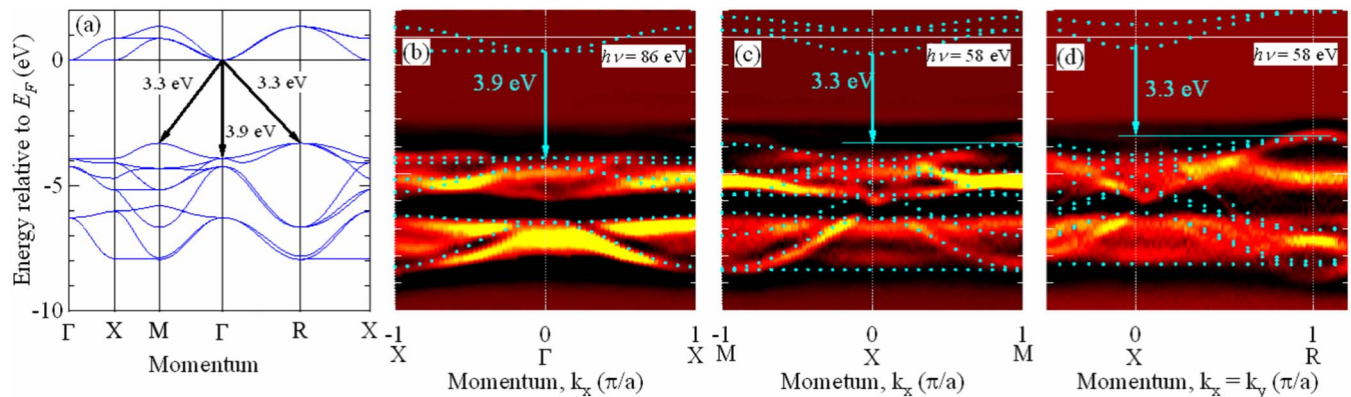


FIG. 3. (Color online) Comparison between the ARPES band structure and TB calculation, (a) Band structure of STO. [(b)-(d)] Comparison for the Γ -X, the X-M, and the X-R directions. The direct and indirect gaps are indicated. The TB calculation has reproduced the experimental ARPES band structure except for the overall shifts of the O 2p band by ~ 500 meV.

- ¹M. Imada, A. Fujimori, and Y. Tokura, *Rev. Mod. Phys.* **70**, 1039 (1998).
- ²R. J. O. Mossaneck, M. Abbate, and A. Fujimori, *Phys. Rev. B* **74**, 155127 (2006).
- ³Y. Ishida, R. Eguchi, M. Matsunami, K. Horiba, M. Taguchi, A. Chainani, Y. Senba, H. Ohashi, H. Ohta, and S. Shin, *Phys. Rev. Lett.* **100**, 056401 (2008).
- ⁴D. Goldschmidt and H. L. Tuller, *Phys. Rev. B* **35**, 4360 (1987).
- ⁵K. van Benthem, C. Elsässer, and R. H. French, *J. Appl. Phys.* **90**, 6156 (2001).
- ⁶J. F. Schooley, W. R. Hosler, and M. L. Cohen, *Phys. Rev. Lett.* **12**, 474 (1964).
- ⁷C. S. Koonce, M. L. Cohen, J. F. Schooley, W. R. Hosler, and E. R. Pfeiffer, *Phys. Rev.* **163**, 380 (1967).
- ⁸L. F. Mattheiss, *Phys. Rev. B* **6**, 4718 (1972).
- ⁹L. F. Mattheiss, *Phys. Rev.* **181**, 987 (1969).
- ¹⁰A. H. Kahn and A. J. Leyendecker, *Phys. Rev.* **135**, A1321 (1964).
- ¹¹Y. Haruyama, S. Kodaira, Y. Aiura, H. Bando, Y. Nishihara, T. Maruyama, Y. Sakisaka, and H. Kato, *Phys. Rev. B* **53**, 8032 (1996).
- ¹²Y. Aiura, I. Hase, H. Bando, T. Yasue, T. Saitoh, and D. S. Dessau, *Surf. Sci.* **515**, 61 (2002).
- ¹³M. Kawasaki, K. Takahashi, T. Maeda, R. Tsuchiya, M. Shinohara, O. Ishiyama, T. Yonezawa, M. Yoshimoto, and H. Koinuma, *Science* **266**, 1540 (1994).
- ¹⁴K. Horiba, H. Ohguchi, H. Kumigashira, M. Oshima, K. Ono, N. Nakagawa, M. Lippmaa, M. Kawasaki, and H. Koinuma, *Rev. Sci. Instrum.* **74**, 3406 (2003).
- ¹⁵H. Wadati, T. Yoshida, A. Chikamatsu, H. Kumigashira, M. Oshima, H. Eisaki, Z. X. Shen, T. Mizokawa, and A. Fujimori, *Phase Transit.* **79**, 617 (2006).
- ¹⁶J. C. Slater and G. F. Koster, *Phys. Rev.* **94**, 1498 (1954).
- ¹⁷W. A. Harrison, *Electronic structure and the properties of solids* (Dover, New York, 1989).
- ¹⁸T. Yoshida (unpublished).
- ¹⁹L. Perfetti, H. Berger, A. Reggiani, L. Degiorgi, H. Höchst, J. Voit, G. Margaritondo, and M. Grioni, *Phys. Rev. Lett.* **87**, 216404 (2001).
- ²⁰K. M. Shen, F. Ronning, D. H. Lu, W. S. Lee, N. J. C. Ingle, W. Meevasana, F. Baumberger, A. Damascelli, N. P. Armitage, L. L. Miller, Y. Kohsaka, M. Azuma, M. Takano, H. Takagi, and Z. X. Shen, *Phys. Rev. Lett.* **93**, 267002 (2004).
- ²¹H. Wadati, A. Chikamatsu, M. Takizawa, R. Hashimoto, H. Kumigashira, T. Yoshida, T. Mizokawa, A. Fujimori, M. Oshima, M. Lippmaa, M. Kawasaki, and H. Koinuma, *Phys. Rev. B* **74**, 115114 (2006).
- ²²G. D. Mahan, *Many-Particle Physics* (Plenum, New York, 1981).
- ²³H. Kawazoe, M. Yasukawa, H. Hyodo, M. Kurita, H. Yanagi, and H. Hosono, *Nature (London)* **389**, 939 (1997).